Biointerface Research in Applied Chemistry
Open-Access Journal (ISSN: 2069-5837)

Article
Volume 15, Issue 3, 2025, 31
https://doi.org/10.33263/BRIAC153.031

An In-silico Analysis of the Targeting of Cyclooxygenase-2, Lipoxygenases, and Glutathione S-transferase, Major Components of the Flesh of the Snail *Helix aspersa* Müller, Using a Molecular Docking: Research Focused on Colorectal Cancer

Marouane Aouji [1,*], Malak Zirari [2], Amine Rkhaila [3] Rachid Bengueddour [1]

[1] Laboratory of Natural Resources and Sustainable Development, Department of Biology, Faculty of Sciences, Ibn Tofail University, BP 133, Kenitra 14000, Morocco; aouji.marouane@uit.ac.ma (M.A.); rachid.bengueddour@uit.ac.ma (R.B.);
[2] Laboratory of Organic Chemistry Catalysis and Environment, Department of Chemistry, Faculty of Sciences, Ibn Tofail University, BP 133, Kenitra 14000, Morocco; malak.zirari@uit.ac.ma (M.Z.);
[3] Laboratory of Biotechnology, Agri-food, Materials and Environment, Department of Biology, Faculty of Science and Technology - Mohammedia, Hassan II University, BP 146, Casablanca 28806, Morocco; amine.rkhaila@uit.ac.ma (A.R.);
* Correspondence: aouji.marouane@uit.ac.ma;

Received: 5.04.2025; Accepted: 11.05.2025; Published: 7.06.2025

Abstract: A cumulative accumulation of genetic and epigenetic abnormalities affecting the epithelial cells of the colon and/or the rectum causes colorectal cancer (CCR), a major cancer on a global scale. This study uses an in silico molecular docking approach to investigate the potential therapeutic benefits of bioactive extracts from the flesh of *Helix aspersa* Müller in the treatment of CCR. The toxicological analysis revealed that the chosen compounds had an acceptable safety profile with no adverse effects on hepatotoxicity, cardiotoxicity, or nephrotoxicity. The ADMET and biodisponibility investigations verified that all ligands met Lipinski's criteria, indicating their potential as drug candidates. Pharmacokinetic properties have shown that some compounds, such as octanoic acid and hexadecanoic acid, have high gastrointestinal absorption and the ability to pass through the blood-brain barrier, which may be advantageous for some applications. Evaluation of the liaison energies and inhibition constants between the ligands and the target proteins has been made possible by molecular docking. The findings demonstrated that for all target proteins, the most negative interaction energies and the lowest inhibition constants were provided by (3β)-Cholest-5-en-3-ol and Cholest-4-en-3-one, indicating a strong affinity and a high potential inhibitor. Through hydrogen, alkyl, and pi-sigma bonds, these two compounds have also shown persistent interactions with key residues of the protein's active regions. Octanoic acid, on the other hand, has demonstrated the least affinity and the least amount of inhibitory power.

Keywords: CCR; *Helix aspersa* Müller; molecular docking.

1. Introduction

Malignant diseases known as colorectal cancer (CCR) are characterized by the anarchic proliferation of glandular epithelial cells in the colon and/or the rectum. According to data from the World Health Organization, it is the third most diagnosed cancer and the second leading cause of death globally, making it a significant public health concern. Three main subtypes

have been identified: sporadic, inherited and linked to a chronic inflammatory condition [1]. According to Eng and Hochster [2], the incidence of this disease is still rising globally, with a noteworthy trend among young people in industrialized nations.

The established risk factors include certain lifestyle factors, such as imbalanced eating, sedentary lifestyles, excessive alcohol and tobacco use, genetic predispositions, and chronic pro-inflammatory conditions [3]. According to Ferlay et al. [4], 9.4% of cancer-related deaths in the environment were directly related to CCR.

The identification and management of modifiable risk factors play a critical role in primary prevention. Interventions based on improving lifestyle choices, such as increasing physical activity, adopting a healthy diet, and using preventive medications like aspirin, have been shown to be effective in lowering the incidence of CCR. In addition, systematic screening that enables the early detection and removal of precancerous lesions remains a crucial secondary strategy to slow the disease's progression [5-7].

There is ample evidence linking the CCR to chronic inflammatory bowel diseases like Crohn's disease and hemorrhagic rectocolitis. This link would be supported by accelerated cellular renewal and an increase in sporadic mutations brought on by persistent intestinal mucus inflammation [8].

The resistance to chemotherapeutic regimens seen in the majority of individuals with metastatic CCR represents another significant therapeutic challenge. Despite significant advancements in modern treatments that have improved global survival, pharmacological resistance continues to be a major barrier limiting the effectiveness of current strategies [9,10].

The current treatment of CCR is based on a multimodal approach that combines surgery, chemotherapy, targeted therapy, immunotherapy, and genetic therapy. The standard chemotherapeutic schemes, such as FOLFOX and CAPIRI, are frequently supplemented by specific targeted agents, such as Cetuximab or Bevacizumab, that interfere with key molecular pathways involved in tumor growth. Immunotherapy, including by inhibitors of immune control points (Pembrolizumab, Nivolumab), offers promising prospects for restoring the antitumoral immune response. Newly emerging approaches, such as adoptive T lymphocyte therapy and cytokine-based therapies, are actively being investigated to overcome the limitations of conventional treatments [11].

In this regard, natural products play a significant role in the search for new therapeutic options [12]. Approximately 50% of anticancer agents currently on the market are natural or derived from biodiversity-derived compounds [13,14]. These include various classes of biomolecules, such as alkaloids, polyphenols, polysaccharides, and diterpenoids, each of which has unique pharmacological characteristics.

The current study aims to investigate the potential of CCR inhibitors of natural bioactive compounds extracted from the flesh of *Helix aspersa* Müller. Using an in silico molecular docking approach, we assessed the interactions between three key proteins implicated in the physiopathology of CCR: glutathione S-transferase (GST), cyclooxygenase-1 (COX-1), and lipoxygenases (LOX), and seven bioactive compounds (L_1-L_7). This research may reveal new natural ligands that can block harmful pathogenic pathways, providing novel insights into the creation of alternative therapies for treating CCR.

2. Materials and Methods

2.1. Preparation of ligands.

According to our previous scientific research [15], seven bioactive compounds present in the snail flesh *Helix aspersa* Müller have been identified and chosen as ligands. The corresponding structures were extracted from the PubChem-NCBI database in 3D SDF format (Figure 1). PyMOL was used to convert the ligands from the SDF files to the Protein Data Bank (PDB) format, and the ligand molecules were downloaded separately in the AutoDock tools before being saved in the pdbqt format.

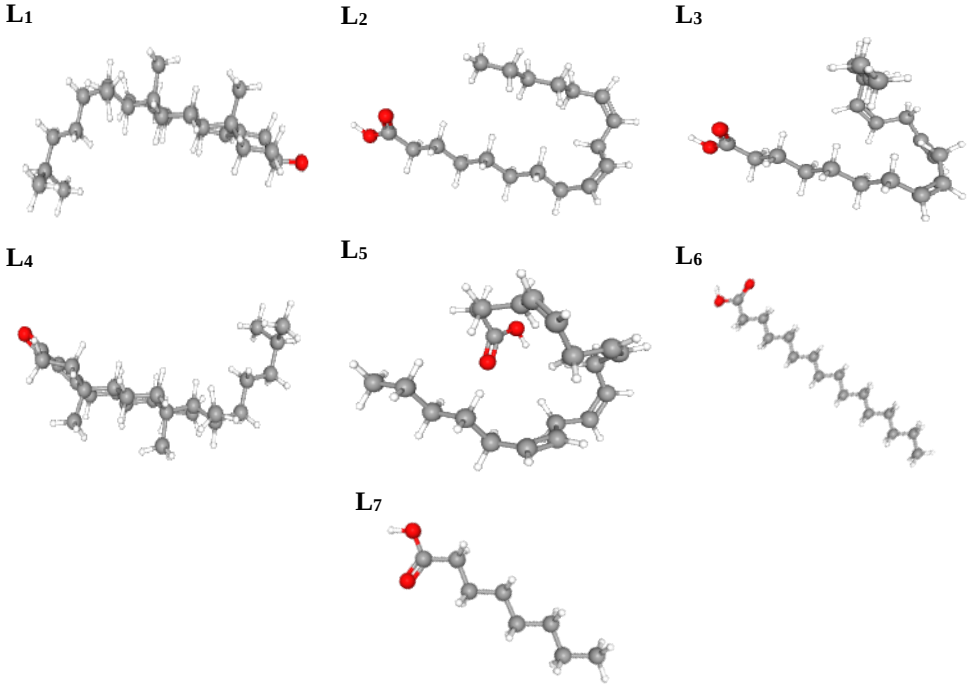

Figure 1. 3D structure of the ligands. (3β)-Cholest-5-en-3-ol **(L1)**; (Z,Z) 9,12-Octadecadienoic acid: (**L2)**; 8,11,14-Eicosatrienoic acid: (**L3)**; Cholest-4-en-3-one: (**L4)**; cis-5,8,11,14-Eicosatetraenoic acid: (**L5)**; Hexadecanoic acid (**L6)**; Octanoic acid (**L7)**.

2.2. Toxicity analysis.

The toxicity evaluation was conducted using Web ProTox-III [16], a program that is crucial for the development of new drugs because it predicts the toxicity of small molecules. The toxicity analysis carried out in this study took into consideration a number of factors, including the LD_{50}, the estimated class of toxicity, immunotoxicity, neurotoxicity, hepatotoxicity, mutagenicity, carcinogenicity, and cytotoxicity.

2.3. ADMET studies.

The ADMET analysis (adsorption, distribution, metabolism, excretion, and toxicity) is crucial to establish the pharmacodynamic characteristics of the molecule. SWISSADME, a web-based online server, was used to identify the therapeutic properties of natural compounds and drugs with the most likely matches [17]. In SWISSADME, the smiles of the ligands have been retrieved from PubChem.

2.4. Preparation of proteins.

The Protein Database (PDB) provided the crystalline structures of glutathione S-transferase (PDB ID: 7XBA), lipoxygenase-2 (PDB ID: 7LAF), and COX-1 (PDB ID: 6Y3C) (Figure 2). It was then incorporated into AutoDock, a molecular docking program. Using the Biovia Discovery Studio 2024 software (Accelrys, San Diego, CA, USA), the protein was first prepared by removing the ligand molecule from the active site. Next, the water molecules were removed in accordance with the indications found in the literature [18-20]. Then, hydrogen atoms were added to the enzyme structures using AutoDockTools 4.2.6 version 1.5.7. Partial atomic charges (Kollman charges) were then applied to the macromolecule, and it was turned into a PDBQT file.

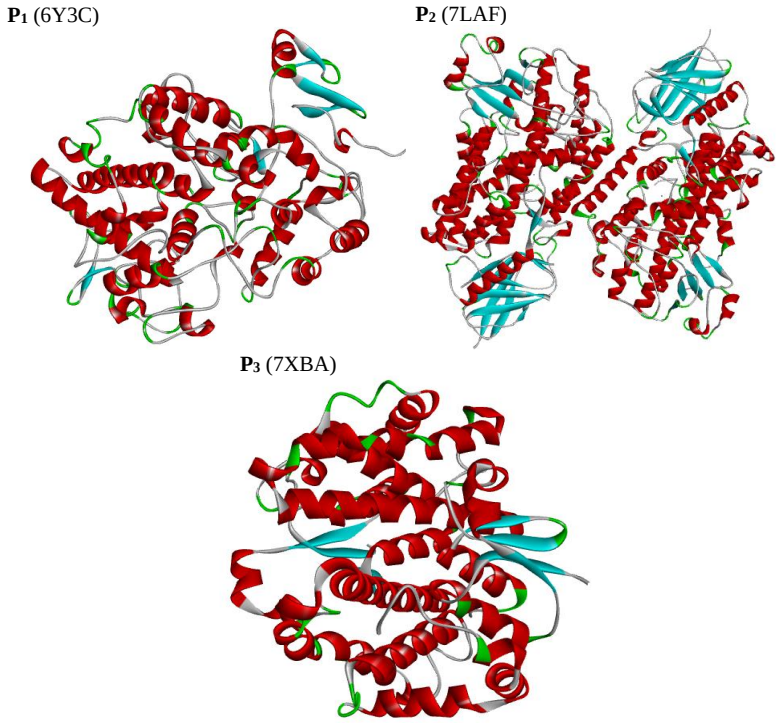

Figure 2. 3D structure of the proteins. **7XBA**: glutathione S-transferase, **7LAF**: lipoxygenase-2, and **6Y3C**: COX-1.

2.5. Molecular docking analysis.

In order to define the areas of interest in the enzyme, the AutoGrid software was used to perform docking calculations [21] using the genetic algorithm and the local search parameters (LGA). The standard script method was used to perform the molecular bond analysis of all the chosen bioactive compounds using AutoDock Vina [22]. The grid's dimensions were recorded in a file in the config format.txt.

The following parameters were used to create a mesh centered on the protein's co-crystallized ligands: a mesh spacing of 0.500, a resolution of 60 Å 60 Å 60 Å points, and coordinates x=-36.654, y=-51.733, z=2.080; x=-46.971, y=6.523, z=532.310; x=21.787, y=-22.229, z=-24.301, respectively, for COX-1, LOX, and GST.

The Biovia discovery lab (Ver. 2024) has been used to study the fixed positions of complex structures and the aminated acids that interact.

3. Results and Discussion

3.1. Toxicity analysis.

Toxicity features were studied using ProTox-III. The prediction models are constructed from investigations carried out in vitro (Tox21 tests, bacterial mutation experiments of Ames, HepG2 cytotoxicity tests, and immunotoxicity tests) and in vivo (carcinogenicity, hepatotoxicity) (Table 1).

Table 1. Toxicity analysis of biocompounds.

L. No	LD_{50} / toxicity class	Nephr	Hepat	Carcin	Card	Imm	Cyto	Neur
L_1	890mg/kg; 4	0.92	0.85	0.51	0.81	0.99	0.95	0.51
L_2	10000mg/kg; 6	0.91	0.55	0.55	0.99	0.96	0.71	0.91
L_3	10000mg/kg; 6	0.55	0.55	0.64	0.99	0.96	0.71	0.91
L_4	2300mg/kg; 5	0.91	0.77	0.57	0.83	0.99	0.81	0.56
L_5	10000mg/kg; 6	0.55	0.55	0.64	0.99	0.98	0.71	0.91
L_6	900mg/kg; 4	0.53	0.52	0.63	0.99	0.99	0.74	0.92
L_7	900mg/kg; 4	0.53	0.52	0.63	0.99	0.99	0.74	0.92

Hepat: Hepatotoxicity; Carcin: Carcinogenicity; Neur: Neurotoxicity; Imm: Immunotoxicity; Cytot: Cytotoxicity; Nephr: Nephrotoxicity; Card: Cardiotoxicity.

The bioactive compounds chosen for this study have not been found to be unreliable in terms of nephrotoxicity, hepatotoxicity, cardiotoxicity, or cytotoxicity. Similarly, L_1 has shown a dynamic activity in terms of carcinotoxicity, neurotoxicity, and immunotoxicity, and a noteworthy activity of L_4 has been observed in terms of neurotoxicity and immunotoxicity. The table shows the problems expected by the toxicity evaluation.

3.2. ADMET analysis.

All of the biocomposés met most of the parameters; therefore, the seven substrates met Lipinski's five criteria and were put through coupling studies (Table 2).

Table 2. Dependent variables of chemical compounds.

L. No	PubChem ID	LogP	MW	nOH	nOHNH	Nb	Nb viol	Mol ref
L_1	5997	7.39	386.65	1	1	5	1	123.61
L_2	5280450	5.88	280.45	2	1	14	1	89.46
L_3	5280581	6.44	306.48	2	1	15	1	98.60
L_4	91477	7.60	384.64	1	0	5	1	122.65
L_5	444899	6.22	304.47	2	1	14	1	98.13
L_6	985	5.55	256.42	2	1	14	1	80.80
L_7	379	2.43	144.21	2	1	6	0	42.34

LogP: lipophilicity; Mol Wt: molecular weight; nOH: no. of H bond acceptors; nOHNH: no. of H bond donors; Nb: no. of rotatable bonds; Nb viol: no of violations; Mol ref: molecular refractivity.

A compound's hydrophobicity is represented by logP; a high lipophilicity shown by a considerable logP (logP >5) will probably improve the permeability of the membranes, but it can also result in lowered water solubility. High values for L_1 (7.39), L_3 (6.44), and L_4 (7.60) point to a high lipophilicity that would enhance the bridging of membranes while perhaps affecting solubility. Still, L_7 (2.43) has the lowest logP, indicating more hydrophilicity, which would probably enhance solubility and lower permeability.

According to Lipinski's rule of five, compounds having a molecular weight less than 500 Da are usually regarded as therapeutic agents. The seven ligands satisfy this requirement; hence, they are possible candidates for the synthesis of medications.

Solubility and bond interactions are influenced by the number of hydrogen bond acceptors (nOH) and donors (nOHNH). L_4 has no hydrogen donors, which could decrease its ability to dissolve and interact. On the other hand, L_2, L_6, and L_7 have two hydrogen atoms that are bond donors, suggesting an ability to solubilize and interact with biological targets.

Molecular flexibility is influenced by the number of rotating bonds (Nb), which affects the efficiency of the bond. L_3 offers the greatest flexibility (15 rotating links), which gives it the potential ability to adjust to various connection points. L_7 has the lowest score (6), which indicates that it is more rigid.

Molecular refractivity (Mol ref), which denotes the polarizability of a molecule, influences its solubility and interactions. L_1 and L_4 display the greatest refractivity (123.61), suggesting intense interactions. L_7 has the lowest score (42.34), indicating a lower interaction potential.

3.3. Pharmacokinetic analysis and ligand comparisons.

The in silico pharmacokinetic profile of the ligands, as illustrated in Table 3, emphasizes that the drug similarity and the pharmacokinetic characteristics of certain compounds resemble those of the drugs already marketed.

Table 3. *In silico* pharmacokinetics of ligands using SwissADME.

L. No	ESOL (Log S)	GIads	BBB	P-gp	Cytochromes				
					3A4	1A2	2C19	2C9	2D6
L_1	–7.40 (PS)	Low	No	No	No	No	No	Yes	No
L_2	–7.40 (PS)	Low	No	No	No	No	No	Yes	No
L_3	–7.40 (PS)	Low	No	No	No	No	No	Yes	No
L_4	–7.17 (PS)	Low	No	No	No	No	No	Yes	No
L_5	–7.17 (PS)	Low	No	No	No	No	No	Yes	No
L_6	–5.02 (PS)	High	Yes	No	No	Yes	No	Yes	No
L_7	–2.26 (S)	High	Yes	No	No	No	No	No	No

Table 3 lists the results of the ADME prediction for the seven compounds, including the cutaneous permeability value, the gastrointestinal absorption, the permeability of the BBB, the P-glycoprotein substrate, the inhibition capacity, and the substrate of the cytochrome P450 enzyme derived from the SwissADME prediction.

The ESOL Log S values represent the ability of the ligands to dissolve. Lower (more negative) values indicate a lower solubility. L_1 to L_6 has a very low solubility (–7.40 to –7.17), indicating their low dissolution capacity (PS). This could influence their bioavailability. L_7 (–2.26) has a higher solubility, being classified as soluble (S).

It is likely that the ligands having a high gastrointestinal absorption are effectively assimilated at the intestinal level. L_6 and L_7 have a high absorption capacity, which makes them more promising for oral bioavailability. The others (L_1-L_5) have low absorption, which could limit their effectiveness as oral treatments.

L_6 and L_7 have the ability to cross the Blood-brain Barrier, which indicates that they could exert an action at the level of the central nervous system. L_1-L_5 do not cross the blood-brain barrier, which limits their potential use in central nervous system applications.

The P-gp is a transporter that expels drugs out of cells, influencing the preservation of drugs. None of the ligands act as a substrate for P-gp, which indicates that they are not likely to be expelled, which is conducive to bioavailability.

CYP enzymes, present in the liver, intervene in the metabolism of drugs by influencing their degradation and elimination. CYP3A4: only L_6 is interacting, indicating that it could be

metabolized quickly. CYP1A2: L6 indicates an interaction, suggesting possible impacts on the metabolism of drugs. CYP2C19: no ligands show interaction with this enzyme, which indicates a low probability of its metabolization. CYP2C9: an interaction between L_1 and L_5 suggests a potential metabolism by this enzyme. CYP2D6: only the L_1 is affected, which could have an impact on its pharmacokinetics.

The interaction of cytochrome P450 isoenzymes with drugs can lead either to an accelerated metabolism when the drug functions as a substrate for a CYP, causing induction, or to an accumulation of the drug when the latter plays the role of inhibitor, thus resulting in inhibition. These two scenarios are generally perceived as having negative consequences [23]. Thus, in the context of drug development, in silico methods to anticipate the interactions between substances or drugs and CYP isoenzymes are of paramount importance.

3.4. Bioavailability radar.

The bioavailability tool offers a quick assessment of the similarity of a compound with an already established pharmaceutical agent. As illustrated in the graph, the magenta area defines the ideal range for each parameter. When analyzing the characteristics of a compound, its radar representation must be located in this magenta zone to be recognized as a drug. Therefore, the ligands must demonstrate oral bioavailability or lack thereof based on their radar representation.

The compound L_7 satisfies the criteria of the radar graph and can therefore, be suggested as being orally bioavailable (Figure 3).

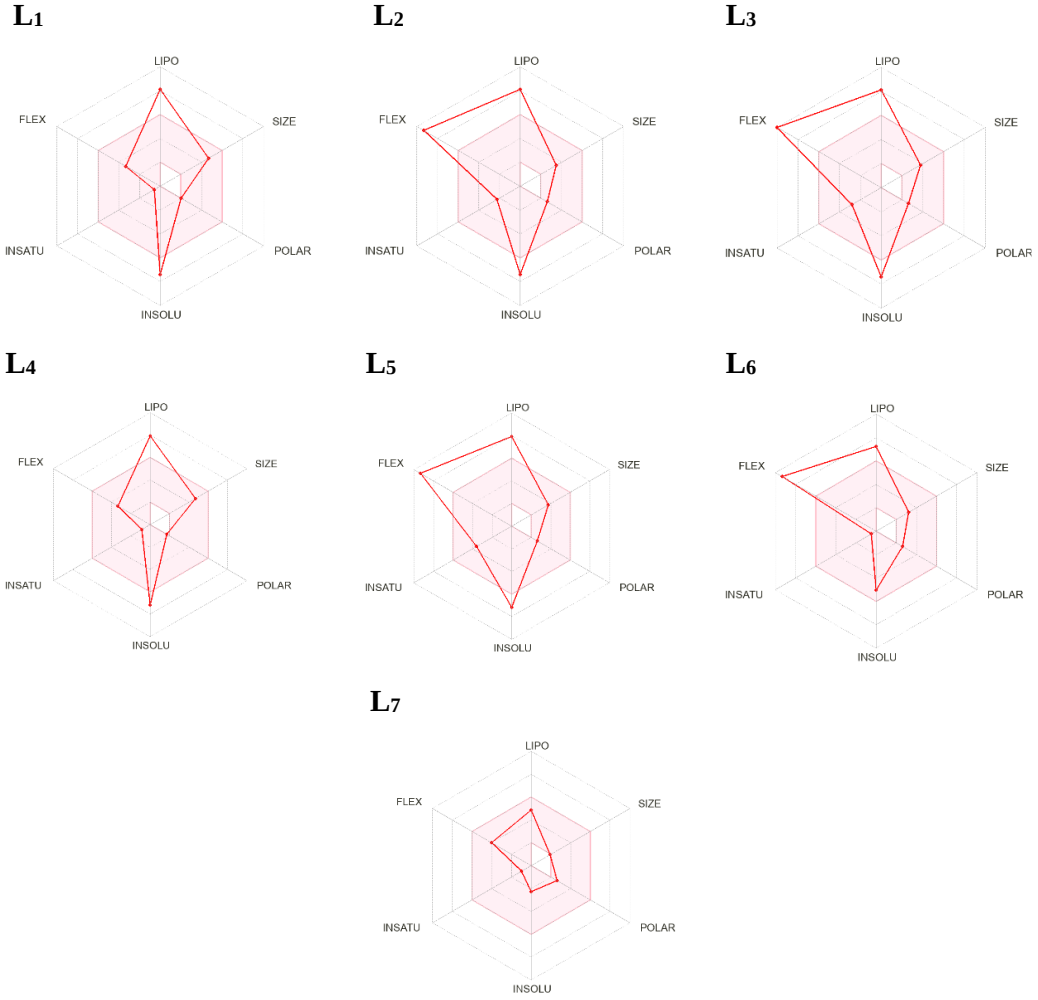

Figure 3. Radar graphs of the ligands.

3.5. Docking analysis.

A molecular docking analysis was carried out on all the ligands filtered from the ADME analysis. The molecular docking computer tool plays a crucial role in drug search. This is done in order to more accurately select possible compounds and examine the creation of bonds at the binding site in the protein-ligand complex. The binding energy influences the binding affinity between ligands and receptors; the lower the energy, the higher the binding affinity [24].

To achieve this goal, seven bioactive compounds were associated with proteins, and their binding energies were compared. The data relating to the binding energy (kcal/mol), to the inhibition constant, and to the amino acids involved in the bonds were recorded following the docking process (Tables 4, 5, and 6).

Table 4. Interaction scores between bioactive compounds and 6Y3C.

L. No	Be (Kcal/mol)	Ic (µM)	Amino acids involved
L_1	−11.45	4.06 nM	Asn A:382; Ala A:202; Ala A:199; Leu A :199; Leu A:390; His A:388; His A:386; Met A:391; His A:207
L_2	−5.28	135.86	Phe A:210; His A:207; Ala A:202; His A:388; Met A: 391; Leu A:390; Ala A:199
L_3	−6.61	14.20	Asn A:382; His A:386; Met A:391; Ala A: 210; Leu A:390; Phe A:210; His A:207; Trp A:387; His A:388; Tyr A:385; Ala A:199
L_4	−11.27	5.52 nM	Ala A:202; Ala A:199; Tyr A:385; Met A:391; His A:388; Leu A:390; His A:207; Phe A:210; Thr A:212; His A:386
L_5	−6.08	34.83	Gln A:289; Phe A:210; Met A:391; His A:388; Tyr A385; Trp A:387; Ala A:202; Leu A:390; His A:207
L_6	−5.16	165.40	Asn A:382; Thr A:212; His A:207; Phe A:210; Leu A:390; His A:388; His A:386; His A:385
L_7	−4.63	400.67	Arg A:120; Trp A:387; Met A:522; Phe A:518; Ile A523; Val A:349; Ala A:527

Be: Binding energy; Ic: Inhibition constant.

The ligands L_1 and L_4 display the most negative binding energies, respectively, −11.45 and −11.27 Kcal/mol, as well as the lowest Ic values, namely 4.06 nM and 5.52 nM. This means they have the greatest affinity towards the target protein and are the most powerful inhibitors. The ligands L_2, L_3, L_5, L_6, and L_7 have less negative binding energies as well as higher Ic, indicating lower affinity and inhibition. The L_7 ligand has the lowest affinity and the most modest inhibitory power.

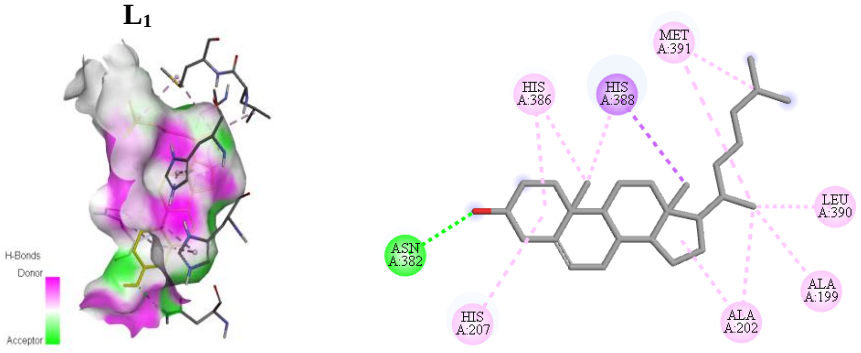

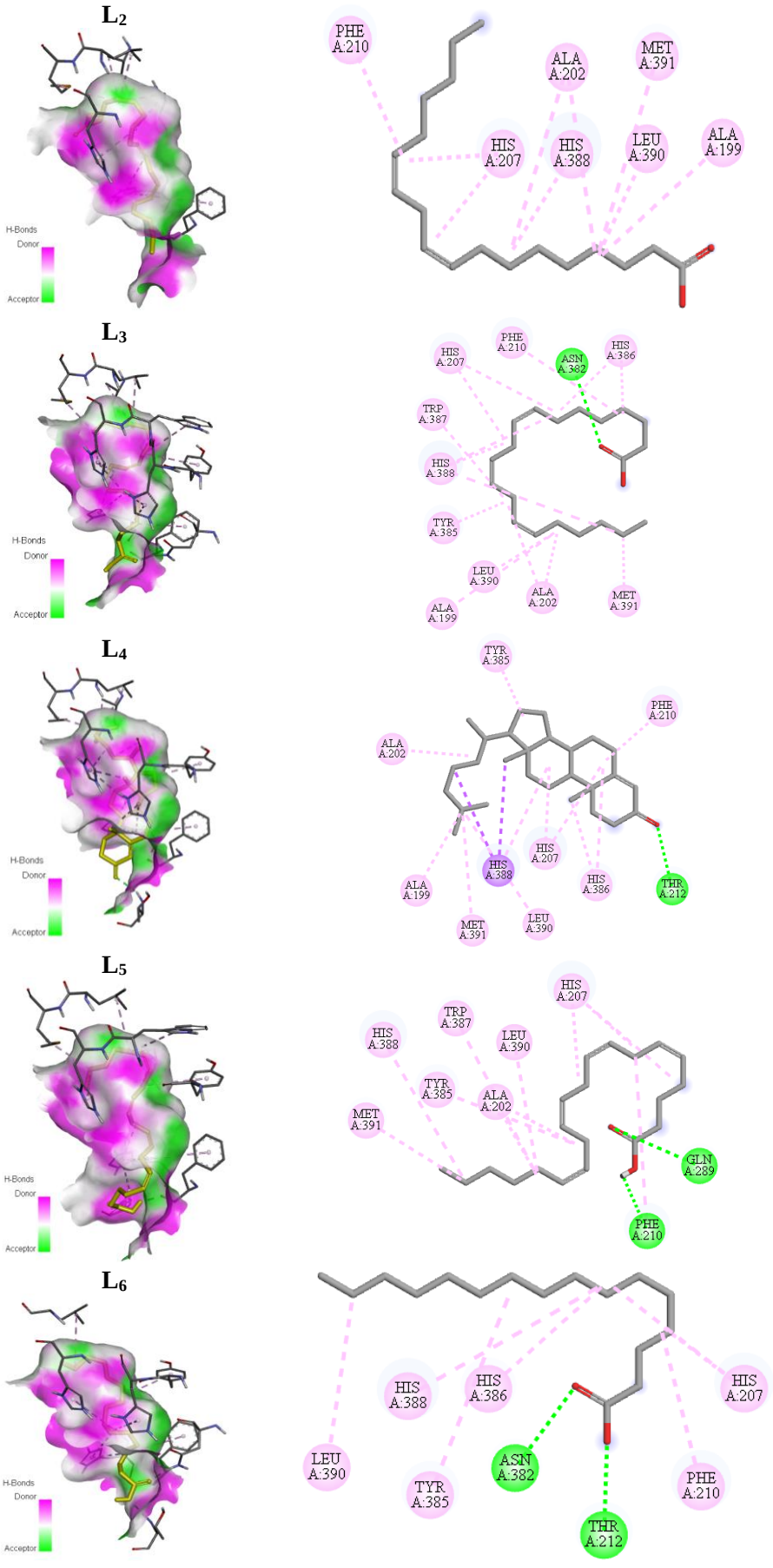
L2
PHE A:210
ALA A:202
MET A:391
HIS A:207
HIS A:388
LEU A:390
ALA A:199
H-Bonds
Donor
Acceptor
L3
PHE A:210
HIS A:207
ASN A:382
HIS A:386
TRP A:387
HIS A:388
TYR A:385
LEU A:390
ALA A:202
ALA A:199
MET A:391
H-Bonds
Donor
Acceptor
L4
TYR A:385
PHE A:210
ALA A:202
HIS A:207
HIS A:388
HIS A:386
THR A:212
ALA A:199
MET A:391
LEU A:390
H-Bonds
Donor
Acceptor
L5
HIS A:207
TRP A:387
HIS A:388
LEU A:390
TYR A:385
ALA A:202
MET A:391
GLN A:289
PHE A:210
H-Bonds
Donor
Acceptor
L6
HIS A:388
HIS A:386
HIS A:207
LEU A:390
ASN A:382
TYR A:385
PHE A:210
THR A:212
H-Bonds
Donor
Acceptor

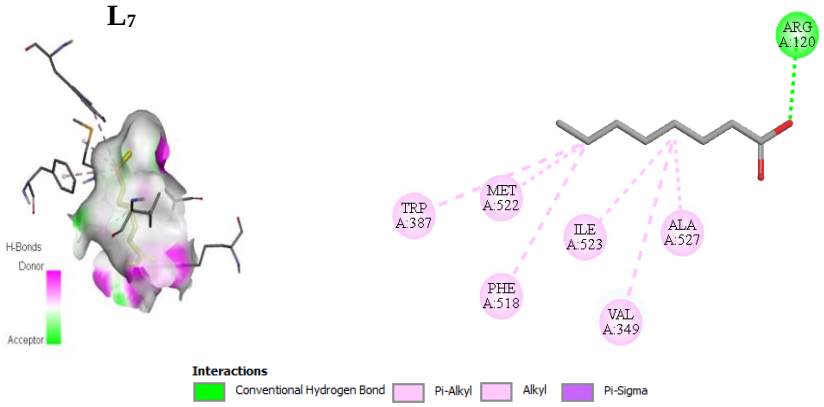

Figure 4. Binding mode of L_1-L_7 compounds with the 6Y3C receptor 3D (left) and 2D (right) views.

The amino acids involved indicate the types of interactions that take place. The results of the molecular docking study showed that the compound L_1 had a hydrogen bond interaction with the protein residues Asn A:382 and an alkyl-type interaction with the protein residues His A:207, His A:386, Leu A:390, Met A:391, Ala A:199 and Ala A:202, and a pi-sigma bond with the protein residues His A:388. In addition, the compound L_4 showed an interaction at the level of a hydrogen bond with the protein residue Thr A:212, as well as eight alkyl bonds with the protein residues Tyr A:385, Phe A:210, Ala A:202, His A:207, His A:386, Leu A:390, Met A:391 and Ala A:199 and a pi-sigma bond with the protein residue His A:388. However, the compound L_7 showed an interaction at one hydrogen bond with the protein residues Arg A:120, and six alkyl bonds with the protein residues Trp A:387, Met A:522, Phe A:518, Ile A523, Val A:349, and Ala A:527 (Table 4, and Figure 4).

Table 5. Interaction scores between bioactive compounds and 7LAF

L. No	Be (Kcal/mol)	Ic (μM)	Amino acids involved
L_1	–10.42	23.17 nM	Ala B:606; Leu B:610; Phe B:184; Leu B:609; Leu B:420; Phe A:192; Leu B:415; Ala B:188; Ala A:193; Ile B:412; Leu B:419; Ala B:416; His B:378
L_2	–5.53	88.40	Ala B:416; Leu B:420; Leu B:419; Phe B:184; Leu B:415; Leu B:610; Gln B:425; His B:378; Arg B:429
L_3	–6.16	30.45	Ala B:188; Leu B:609; Leu B:419; Val B:426; Gln B:425; Phe B:184; Lys A:196; Arg B:429; Leu B:420; Leu B:610; Leu B:415; Ile B:412; Ala B:416
L_4	–11.05	7.99 nM	Leu B:610; Ala B:606; Ala B:188; Leu B:415; Leu B:609; Ile B:412; Leu B:419; Ala B:416; Leu B:420; His B:378
L_5	–5.58	81.12	Ala B:188; Leu B:609; Leu B:605; Ala B:606; Leu B:419; Arg B:429; Leu B:610 Ala B:416; Ile B:412; Leu B:420
L_6	–4.89	259.93	Phe B:184; Leu B:610; Ile A:197; Ala B:188; Lys A:196; Leu B:606; Leu B:419; Ala B:609; Phe A:192; Arg B:429; Val B:426; Leu B:420
L_7	–4.63	400.67	Val B:426; Leu B:419; Leu B:420; Gln B:425; Arg B:429; Leu B:610

Be: Binding energy; Ic: Inhibition constant.

The ligands L_1 and L_4 have the most negative binding energies (–10.42 and –11.05 Kcal/mol, respectively) and the lowest Ic (23.17 nM and 7.99 nM). This indicates they have the highest affinity for the target protein and are the strongest inhibitors. The ligands L_2, L_3, L_5, L_6, and L_7 have less negative binding energies and higher Ic, which suggests lower affinity and inhibition. The L_7 ligand is the one with the least affinity and the lowest inhibitory power (Table 5).

L_1

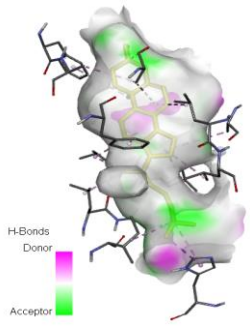
H-Bonds
Donor
Acceptor

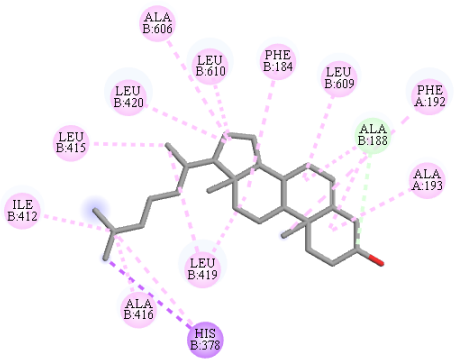
ALA B:606
LEU B:610
PHE B:184
LEU B:609
PHE A:192
LEU B:420
ALA B:188
LEU B:415
ALA A:193
ILE B:412
LEU B:419
ALA B:416
HIS B:378

L_2

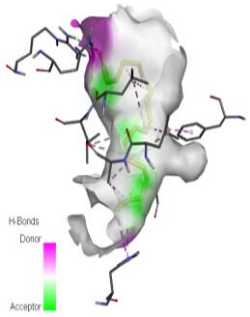
H-Bonds
Donor
Acceptor

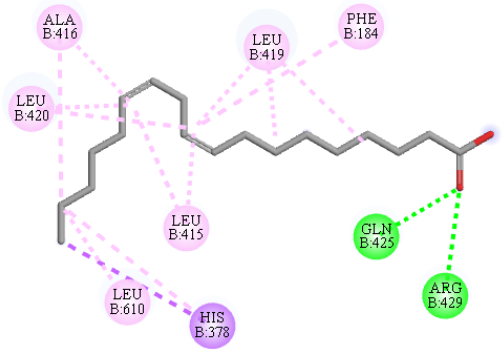
ALA B:416
LEU B:419
PHE B:184
LEU B:420
LEU B:415
GLN B:425
ARG B:429
LEU B:610
HIS B:378

L_3

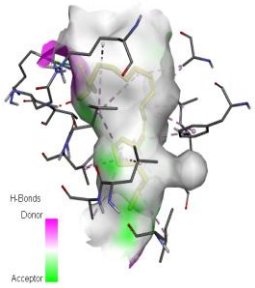
H-Bonds
Donor
Acceptor

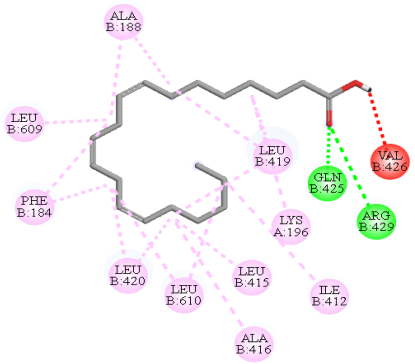
ALA B:188
LEU B:609
LEU B:419
VAL B:426
GLN B:425
PHE B:184
ARG B:429
LYS A:196
LEU B:420
LEU B:610
LEU B:415
ILE B:412
ALA B:416

L_4

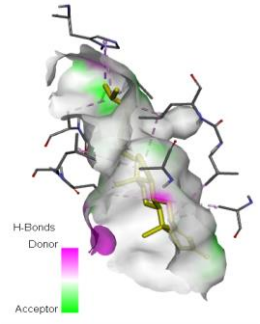
H-Bonds
Donor
Acceptor

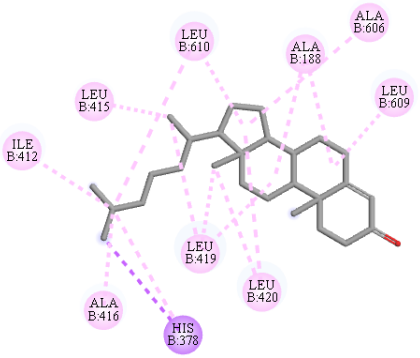
LEU B:610
ALA B:606
ALA B:188
LEU B:415
LEU B:609
ILE B:412
LEU B:419
LEU B:420
ALA B:416
HIS B:378

L_5

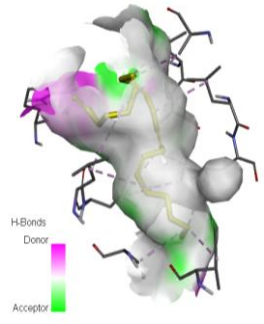
H-Bonds
Donor
Acceptor

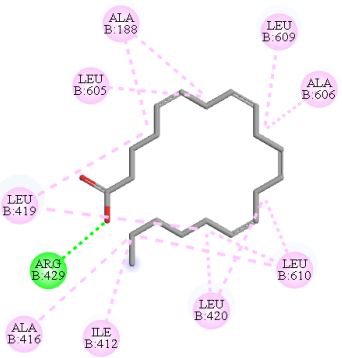
ALA B:188
LEU B:609
LEU B:605
ALA B:606
LEU B:419
ARG B:429
LEU B:610
LEU B:420
ALA B:416
ILE B:412

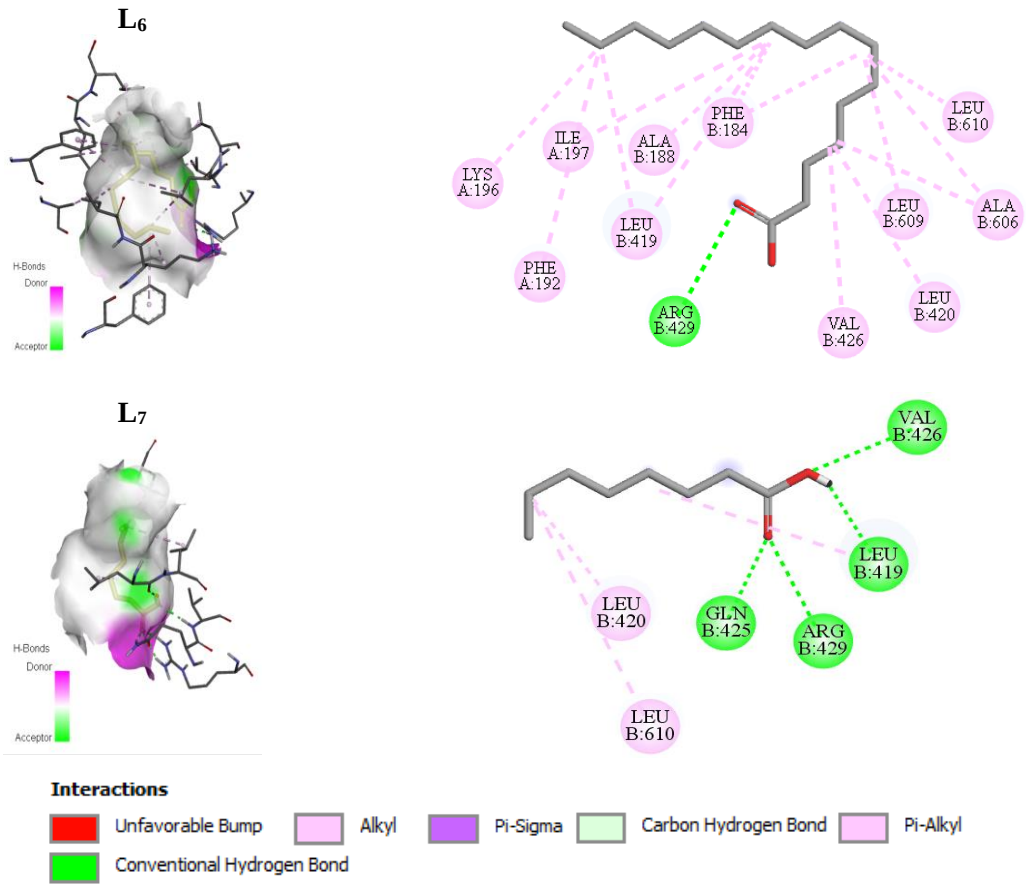

Figure 5. Binding mode of L_1-L_7 compounds with the 7LAF receptor 3D (left) and 2D (right) views.

The results of the molecular docking study showed that the compound L_1 had a pi-sigma bond interaction with the protein residue His B:378, a hydrogen carbon bond with the protein residue Ala B:188, and eleven alkyl-type interactions with the protein residues Ala B:606, Leu B:610, Phe B:184, Leu B:609, Leu B:420, Phe A:192, Leu B:415, Ala A:193, Ile B:412, Leu B:419 and Ala B:416. In addition, the compound L_4 showed an interaction at the level of a carbon-hydrogen bond with the protein residue His B:378, as well as nine alkyl bonds with the protein residues Leu B:610, Ala B:606, Ala B:188, Leu B:415, Leu B:609, Ile B:412, Leu B:419, Ala B:416 and Leu B:420. However, the compound L_7 showed four interactions at a hydrogen bond with the protein residues Val B:426, Leu B:419, Gln B:425, and Arg B:429, and two alkyl bonds with the protein residues Leu B:420 and Leu B:610 (Figure 5).

Table 6. Interaction scores between bioactive compounds and 7XBA.

L. No	Be (Kcal/mol)	Ic (μM)	Amino acids involved
L_1	–7.12	6.00	Tyr A:49; Lys B:102; Arg A:13; Cys B:101; Asp B:98; Cys A:101; Pro A:53
L_2	–3.40	3.23 mM	Pro B:53; Cys B:101; Gln B:51; Arg B:13; Tyr B:49; Tyr B:63
L_3	–3.10	5.32 mM	Leu B:106; Ser B:105; Tyr B:118; Lys B:102; Ala B:121
L_4	–7.30	4.45	Tyr B:49
L_5	–3.97	1.24 mM	Lys B:102; Gln A:51; Pro A:53; Arg A:13; Tyr A:49
L_6	–3.80	1.63 mM	Tyr A:49; Lys B:102
L_7	–4.53	475.21	Arg B:13; Pro B:53

Be: Binding energy; Ic: Inhibition constant

The ligands L_1 and L_4 have the most negative binding energies (–7.12 and –7.30 Kcal/mol, respectively) and the lowest Ic (6.00 μM and 4.45 μM). This indicates they have the highest affinity for the target protein and are the strongest inhibitors. The other ligands have

less negative binding energies and higher Ic (in mM), which suggests lower affinity and inhibition. The L_3 ligand has the least affinity and the lowest inhibitory power (Table 6).

L_1

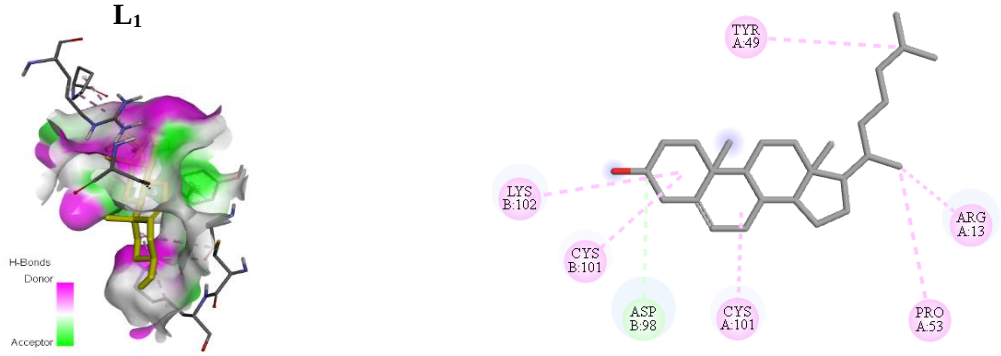

L_2

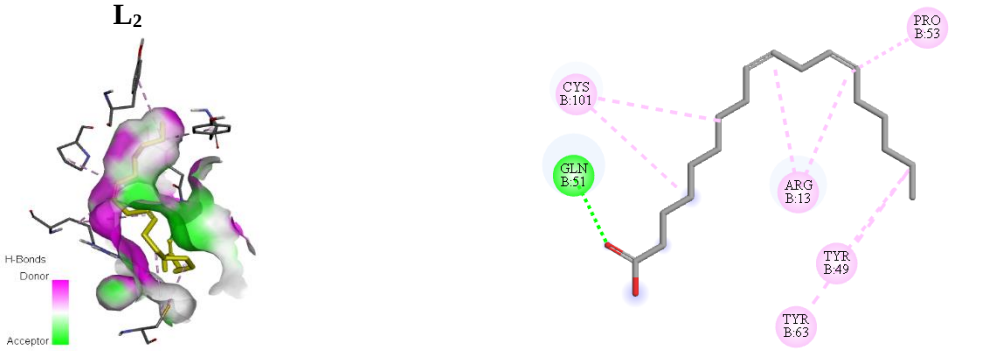

L_3

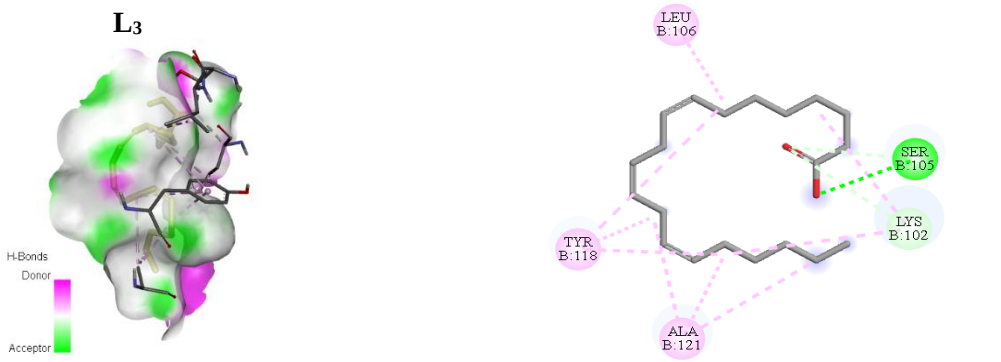

L_4

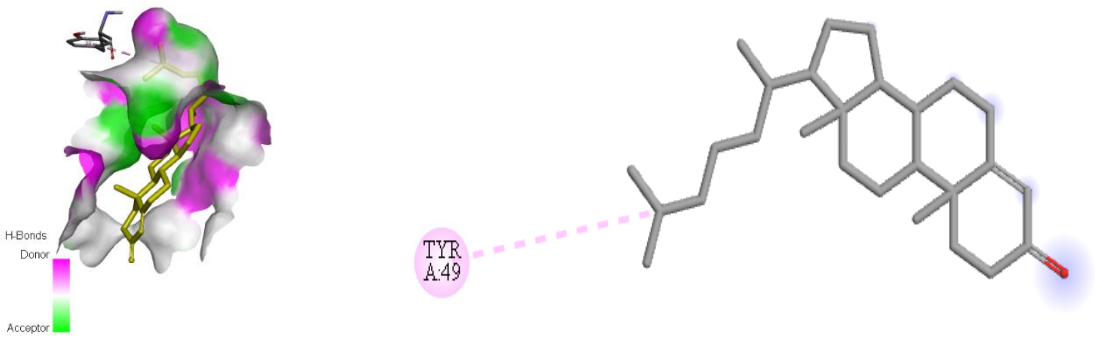

L_5

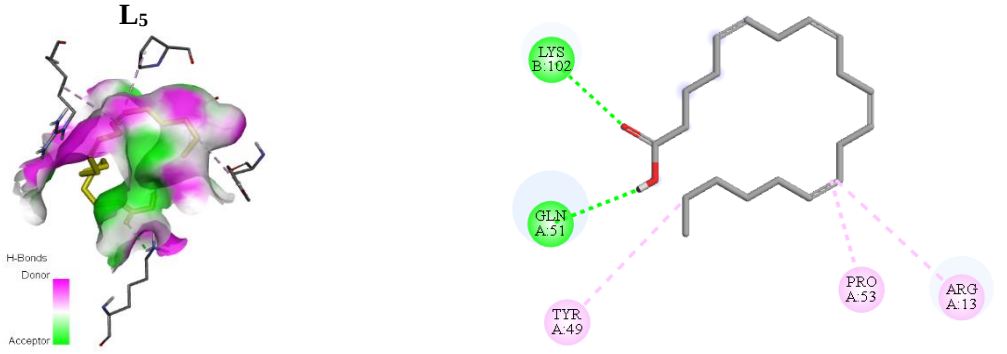

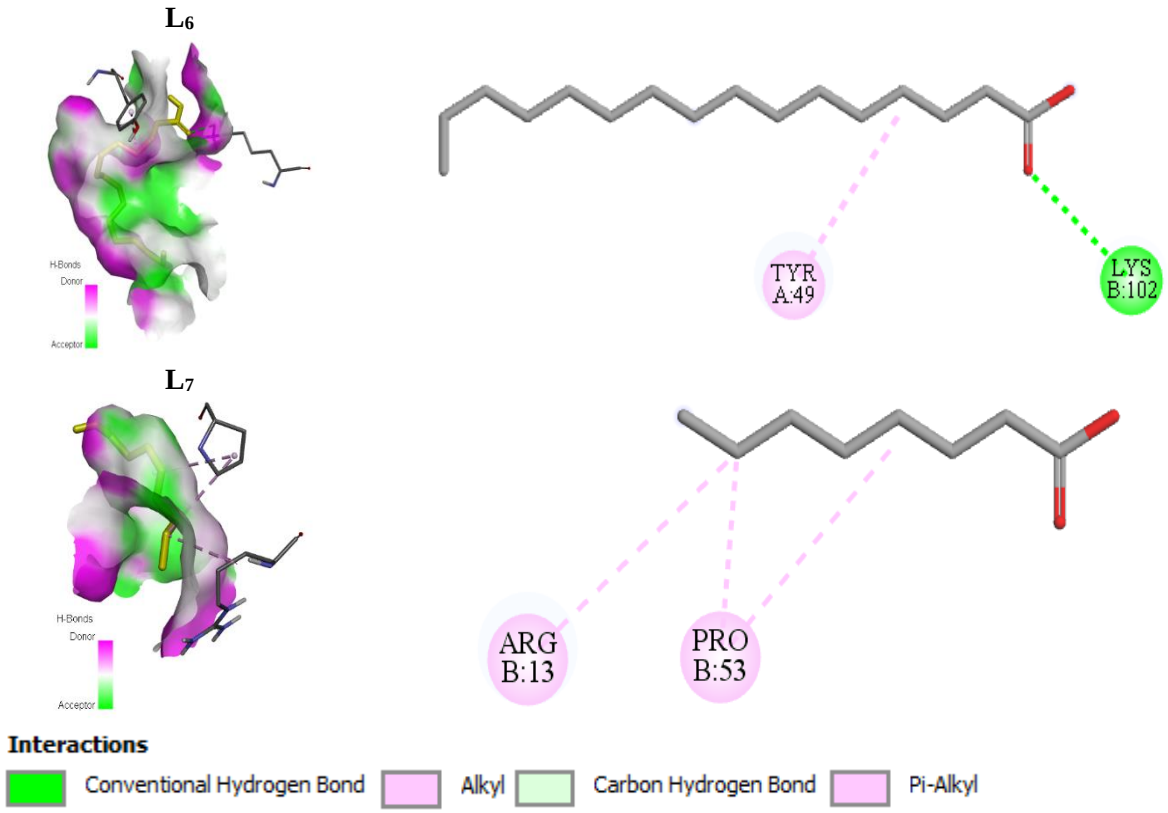

Figure 6. Binding mode of L_1-L_7 compounds with the 7XBA receptor 3D (left) and 2D (right) views

The results of the molecular docking study showed that the compound L_1 had a hydrogen carbon bond with the protein residue Asp B:98 and six alkyl-type interactions with the protein residues Tyr A:49, Lys B:102, Arg A:13, Cys B:101, Cys A:101, and Pro A:53. In addition, the compound L_4 presented an alkyl bond with the protein residues Tyr A:49. However, the compound L_3 showed an interaction at a hydrogen bond with the protein residue Ser B:105, a carbon-hydrogen bond with the protein residue Lys B:102 and three alkyl bonds with the protein residues Leu B:106, Tyr B:118, and Ala B:121 (Figure 6).

The L_1 and L_4 ligands could be promising candidates for developing drugs targeting this protein. A more in-depth study of their interactions and biological effects would be necessary.

4. Conclusions

This study highlights the potential of natural bioactive extracts of *Helix aspersa* Müller as potential inhibitors in treating colorectal cancer. The *in silico* results of this study indicate that the bioactive extracts of the flesh of *Helix aspersa* Müller, specifically (3β)-cholest-5-en-3-ol and Cholest-4-en-3-one, have promising therapeutic potential for the treatment of colorectal cancer. Their strong affinity for the protein targets COX-1, LOX, and GST, along with their safety profile and advantageous pharmacokinetic properties, make them intriguing candidates for creating novel therapeutic approaches. Although these results are encouraging, more in vitro and in vivo experimental research is required to confirm these compounds' biological effectiveness, selectivity, and safety. Furthermore, more research on their mechanisms of action, biodisponibility, and metabolic stability would help to understand their potential in clinical settings better. Thus, this research opens up new avenues for the use of natural products in the creation of alternative treatments for colorectal cancer.

Author Contributions

Conceptualization, M.A., and M.Z.; methodology, M.A.; software, M.A., and M.Z.; validation, M.A., A.R., and R.B.; formal analysis, M.A.; data curation, M.A., and M.Z.; writing—original draft preparation, R.B.; writing—review and editing, A.R., R.B.; supervision, R.B.; All authors have read and agreed to the published version of the manuscript.

Institutional Review Board Statement

Not applicable.

Data Availability Statement

Data supporting the findings of this study are available upon reasonable request from the corresponding author.

Funding

This research received no external funding.

Acknowledgments

The contributors to this work, whether directly or indirectly, have our sincere gratitude.

Conflicts of Interest

The authors declare no conflict of interest.

References

1. Edwards, B.K.; Ward, E.; Kohler, B.A.; Eheman, C.; Zauber, A.G.; Anderson, R.N.; Jemal, A.; Schymura, M.J.; Lansdorp-Vogelaar, I.; Seeff, L.C.; van Ballegooijen, M.; Goede, S.L.; Ries, L.A.G. Annual report to the nation on the status of cancer, 1975-2006, featuring colorectal cancer trends and impact of interventions (risk factors, screening, and treatment) to reduce future rates. *Cancer* **2010**, *116*, 544-573, https://doi.org/10.1002/cncr.24760.
2. Eng, C.; Hochster, H. Early-Onset Colorectal Cancer: The Mystery Remains. *J. Natl. Cancer Inst.* **2021**, *113*, 1608-1610, https://doi.org/10.1093/jnci/djab127.
3. Siegel, R.L.; Wagle, N.S.; Cercek, A.; Smith, R.A.; Jemal, A. Colorectal cancer statistics, 2023. *CA Cancer J. Clin.* **2023**, *73*, 233-254, https://doi.org/10.3322/caac.21772.
4. Data visualization tools for exploring the global cancer burden in 2022. Available online: https://gco.iarc.fr/today (accessed on February 10, **2025**).
5. Rex, D.K.; Boland, R.C.; Dominitz, J.A.; Giardiello, F.M.; Johnson, D.A.; Kaltenbach, T.; Levin, T.R.; Lieberman, D.; Robertson, D.J. Colorectal Cancer Screening: Recommendations for Physicians and Patients from the U.S. Multi-Society Task Force on Colorectal Cancer. *Official journal of the Am. J. Gastroenterol.* **2017**, *112*, 1016-1030, https://doi.org/10.1038/ajg.2017.174.
6. Qaseem, A.; Crandall, C.J.; Mustafa, R.A.; Hicks, L.A.; Wilt, T.J. Screening for Colorectal Cancer in Asymptomatic Average-Risk Adults: A Guidance Statement From the American College of Physicians. *Ann. Intern. Med.* **2019**, *171*, 643-654, https://doi.org/10.7326/M19-0642.
7. Shaukat, A.; Kahi, C.J.; Burke, C.A.; Rabeneck, L.; Sauer, B.G.; Rex, D.K. ACG Clinical Guidelines: Colorectal Cancer Screening 2021. *Am. J. Gastroenterol.* **2021**, *116*, 458–479, https://doi.org/10.14309/ajg.0000000000001122.
8. Peterson, Y.C. Risk factors for colorectal cancer. *MOJ Surg.* **2015**, *2*, 37–42, https://doi.org/10.15406/mojs.2015.02.00015.

9. Dallas, N.A.; Xia, L.; Fan, F.; Gray, M.J.; Gaur, P.; van Buren, G., II; Samuel, S.; Kim, M.P.; Lim, S.J.; Ellis, L.M. Chemoresistant Colorectal Cancer Cells, the Cancer Stem Cell Phenotype, and Increased Sensitivity to Insulin-like Growth Factor-I Receptor Inhibition. *Cancer Res.* **2009**, *69*, 1951-1957, https://doi.org/10.1158/0008-5472.CAN-08-2023.
10. Hu, T.; Li, Z.; Gao, C.-Y.; Cho, C.H. Mechanisms of drug resistance in colon cancer and its therapeutic strategies. *World J. Gastroenterol.* **2016**, *22*, 6876–6889, https://doi.org/10.3748/wjg.v22.i30.6876.
11. Hossain, M.S.; Karuniawati, H.; Jairoun, A.A.; Urbi, Z.; Ooi, D.J.; John, A.; Lim, Y.C.; Kibria, K.M.K.; Mohiuddin, A.K.M.; Ming, L.C.; Goh, K.W.; Hadi, M.A. Colorectal Cancer: A Review of Carcinogenesis, Global Epidemiology, Current Challenges, Risk Factors, Preventive and Treatment Strategies. *Cancers* **2022**, *14*, 1732, https://doi.org/10.3390/cancers14071732.
12. Hossain, S.; Urbi, Z. Effect of Naphthalene Acetic Acid on the Adventitious Rooting in Shoot Cuttings of *Andrographis paniculata* (Burm.f.) Wall. ex Nees: An Important Therapeutical Herb. *Int. J. Agron.* **2016**, *2016*, 1617543, https://doi.org/10.1155/2016/1617543.
13. Huang, X.-m.; Yang, Z.-j.; Xie, Q.; Zhang, Z.-k.; Zhang, H.; Ma, J.-y. Natural products for treating colorectal cancer: A mechanistic review. *Biomed. Pharmacother.* **2019**, *117*, 109142, https://doi.org/10.1016/j.biopha.2019.109142.
14. Newman, D.J.; Cragg, G.M. Natural Products as Sources of New Drugs from 1981 to 2014. *J. Nat. Prod.* **2016**, *79*, 629–661, https://doi.org/10.1021/acs.jnatprod.5b01055.
15. Aouji, M.; Zirari, M.; Imtara, H.; Rkhaila, A.; Bouhaddioui, B.; Mothana, R.A.; Noman, O.M.; Tarayrah, M.; Bengueddour, R. Exploring the Chemical Composition, Antioxidant, and Antibacterial Properties of Helix aspersa Müller Flesh Crude Extract: A Comprehensive Investigation. *ACS Omega* **2024**, *9*, 34754-34764, https://doi.org/10.1021/acsomega.4c04042.
16. Banerjee, P.; Kemmler, E.; Dunkel, M.; Preissner, R. ProTox 3.0: a webserver for the prediction of toxicity of chemicals. *Nucleic Acids Res.* **2024**, *52*, W513-W520, https://doi.org/10.1093/nar/gkae303.
17. Yang, H.; Lou, C.; Sun, L.; Li, J.; Cai, Y.; Wang, Z.; Li, W.; Liu, G.; Tang, Y. admetSAR 2.0: web-service for prediction and optimization of chemical ADMET properties. *Bioinformatics* **2019**, *35*, 1067-1069, https://doi.org/10.1093/bioinformatics/bty707.
18. Trott, O.; Olson, A.J. AutoDock Vina: Improving the speed and accuracy of docking with a new scoring function, efficient optimization, and multithreading. *J. Comput. Chem.* **2010**, *31*, 455–461, https://doi.org/10.1002/jcc.21334.
19. Scapin, G.; Patel, S.B.; Chung, C.; Varnerin, J.P.; Edmondson, S.D.; Mastracchio, A.; Parmee, E.R.; Singh, S.B.; Becker, J.W.; Van der Ploeg, L.H.T.; Tota, M.R. Crystal Structure of Human Phosphodiesterase 3B: Atomic Basis for Substrate and Inhibitor Specificity. *Biochemistry* **2004**, *43*, 6091-6100, https://doi.org/10.1021/bi049868i.
20. Xu, R.X.; Rocque, W.J.; Lambert, M.H.; Vanderwall, D.E.; Luther, M.A.; Nolte, R.T. Crystal Structures of the Catalytic Domain of Phosphodiesterase 4B Complexed with AMP, 8-Br-AMP, and Rolipram. *J. Mol. Biol.* **2004**, *337*, 355-365, https://doi.org/10.1016/j.jmb.2004.01.040.
21. Card, G.L.; England, B.P.; Suzuki, Y.; Fong, D.; Powell, B.; Lee, B.; Luu, C.; Tabrizizad, M.; Gillette, S.; Ibrahim, P.N.; Artis, D.R.; Bollag, G.; Milburn, M.V.; Kim, S.-H.; Schlessinger, J.; Zhang, K.Y.J. Structural Basis for the Activity of Drugs that Inhibit Phosphodiesterases. *Structure* **2004**, *12*, 2233-2247, https://doi.org/10.1016/j.str.2004.10.004.
22. Morris, G.M.; Huey, R.; Lindstrom, W.; Sanner, M.F.; Belew, R.K.; Goodsell, D.S.; Olson, A.J. AutoDock4 and AutoDockTools4: Automated docking with selective receptor flexibility. *J. Comput. Chem.* **2009**, *30*, 2785-2791, https://doi.org/10.1002/jcc.21256.
23. Ji, D.; Xu, M.; Udenigwe, C.C.; Agyei, D. Physicochemical characterisation, molecular docking, and drug-likeness evaluation of hypotensive peptides encrypted in flaxseed proteome. *Curr. Res. Food Sci.* **2020**, *3*, 41-50, https://doi.org/10.1016/j.crfs.2020.03.001.
24. Sarkar, B.; Asad, U.M.; Sajidul, I.S.; Hasanur, R.M.D.; and Araf, Y. Analysis of plant-derived phytochemicals as anti-cancer agents targeting cyclin dependent kinase-2, human topoisomerase IIa and vascular endothelial growth factor receptor-2. *J. Recept. Signal Transduct.* **2021**, *41*, 217-233, https://doi.org/10.1080/10799893.2020.1805628.

Publisher's Note & Disclaimer